Supplementary Materials for

Synthesis and Optical Characterization of Lead-Free Phenylenediammonium Bismuth Halide Perovskites: A Long Charge Carrier Lifetime in Phenylenediammonium Bismuth Iodide

Zumaira Siddique,[1,2,3] Julia L. Payne,[3*] Muhammad T. Sajjad,[4, 5] Natalie Mica,[4] David B. Cordes,[3] Alexandra M. Z. Slawin,[3] Ifor D. W. Samuel,[4] Azhar Iqbal,[1*] John T. S. Irvine.[3*]

[1]Department of Chemistry, Quaid-i-Azam University Islamabad - 45320, Pakistan.

[2]Department of Chemistry, Government College University, Jhang Road Faisalabad, 38000, Pakistan.

[3]EaStCHEM, School of Chemistry, University of St Andrews, North Haugh, St Andrews, KY16 9ST, United Kingdom.

[4]Organic Semiconductor Centre, SUPA, School of Physics and Astronomy, University of St Andrews, North Haugh, St Andrews, KY16 9SS, United Kingdom.

[5]London Centre for Energy Engineering, School of Engineering, London South Bank University, 103 Borough Road, London, SE1 0AA, United Kingdom.

Correspondence should be addressed to Dr Julia L. Payne, jlp8@st-andrews.ac.uk, Dr Azhar Iqbal, aiqbal@qau.edu.pk or Prof. John T.S. Irvine, jtsi@st-andrews.ac.uk.

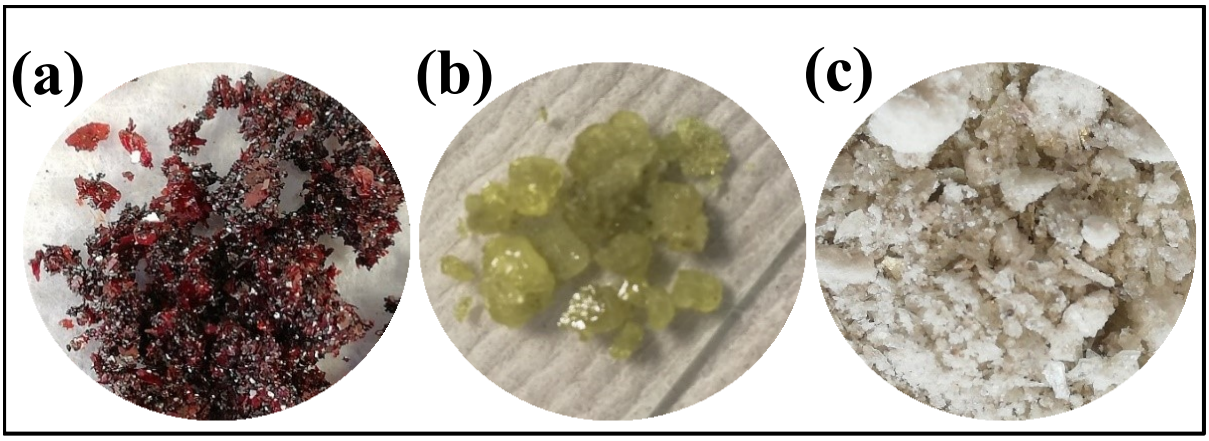

Figure S 1: Photographs of (a) β-$(PPD)_2Bi_2I_{10}$, (b) $(PPD)[BiBr_4]_2 \cdot 2H_2O$ and (c) $(PPD)_2BiCl_7 \cdot H_2O$.

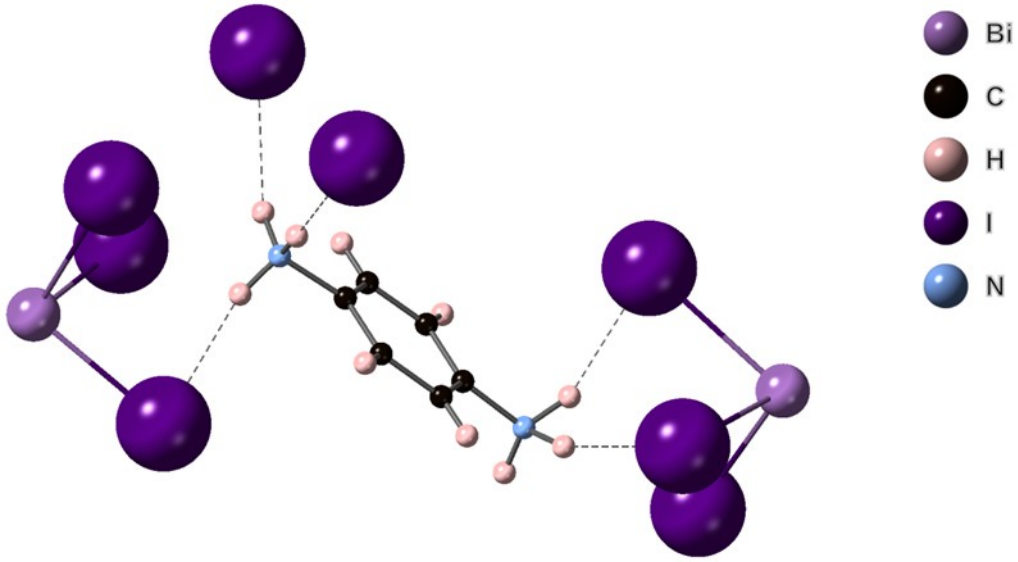

Figure S2: Hydrogen bonding arrangement between *p*-phenylenediammonium (PPD) and iodine atoms from BiI_6 octahedra in $(PPD)BiI_5$. Hydrogen bonds are shown by dashed lines.

Table S 1: Selected structural parameters for structures in the PPD-Bi-I system.

Compound	**$(PPD)(BiI_4)_2I_2$**	**α–$(PPD)_2Bi_2I_{10}$**	**β-$(PPD)_2Bi_2I_{10}$**	**$(PPD)_2Bi_2I_{10}\cdot 4H_2O$**	**$(PPD)BiI_5$**
CSD Ref	1588608	811056	811057	759751	This work
Connectivity of octahedra	Zig-zag chains of edge-sharing BiI_6 octahedra along *a*-axis	Edge-sharing octahedra forming discrete Bi_2I_{10} dimers	Edge-sharing octahedra forming discrete Bi_2I_{10} dimers	Edge-sharing octahedra forming discrete Bi_2I_{10} dimers	Zig-zag chains of corner-sharing BiI_6 octahedra along the *b*-axis
Space group	$P\bar{1}$	$P2_1/c$	$P2_1/n$	$P2_1/n$	$P2_1$
Cell parameters	7.761(1)Å 9.259(1)Å 9.689(1)Å 95.68(3)° 103.19(3)° 93.56(3)°	12.053(5) Å 12.846(7) Å 12.506(6) Å 117.46(5) °	11.4827(3) Å 12.9016(3) Å 14.9698(4) Å 112.40(5) °	11.483(5) Å 12.896(5) Å 14.974(5) Å 112.437(5) °	10.0586(4) Å 8.4358(3) Å 10.8613(5) Å 107.582(4)°
Band gap	1.45 eV	3.01		2.84	
Data collection temperature	100 K	293 K	150 K	293 K	173 K
Bi-I bond lengths	2.9056(6)- 3.3504(6) Å	2.895(3)- 3.182(2) Å	2.923(2)- 3.271(2) Å	2.9204(10)- 3.2706(10) Å	2.9691(5)- 3.3504(6) Å
I-Bi-I bond angles	83.386(6)°- 98.520(17)°	86.22(8) °- 95.55(9) °	87.38(5) °- 91.54(7) °	88.45(4) ° - 91.63(4) °	83.387(8) °- 98.522(17) °-
Bi-Bi distance	4.5122(14) Å	4.770(5) Å	4.563(2) Å	4.5656(15) Å	6.37818(4) Å
Shortest interchain/ intercluster distance	3.871(10) (I4-I2)	3.893(4) (I1-I4)	3.718(4)(3) Å (I3-I5)	3.7253(16) Å (I2-I3)	4.1075 (9) Å (I2-I5)

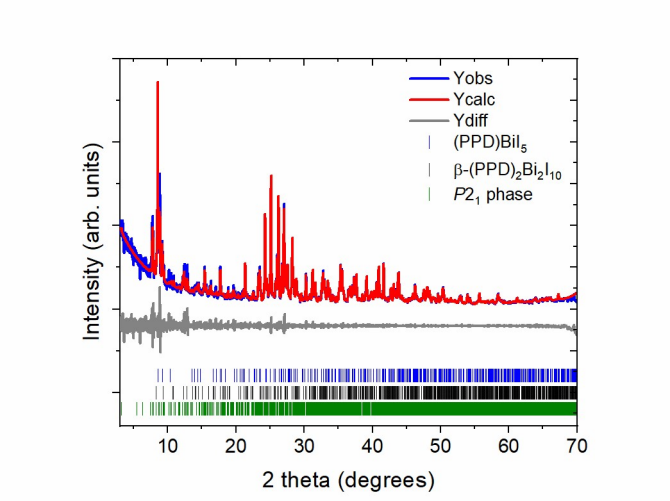

Figure S 3: Pawley fit of the PXRD data for the PPD-Bi-I sample, from which the (PPD)BiI_5 single crystal was isolated. The sample was a mixture of phases including (PPD)BiI_5, β-(PPD)$_2Bi_2I_{10}$ and an unidentified phase, with a monoclinic ($P2_1$) unit cell.

Figure S3 shows the Pawley fit to the PXRD data for the PPD-Bi-I sample, before reaction conditions were optimised. The sample contained a mixture of phases, including an unidentified phase, which preliminary indexing attempts have assigned to space group $P2_1$ and unit cell parameters of a = 27.8952 Å, b = 19.9898 Å, c = 11.9103 Å and β = 85.284°. Unfortunately (PPD)BiI_5 could not be isolated in pure form, so we did not do any further characterisation of this material in terms of UV-Vis, PL or TRPL. Due to the structural diversity of organic ammonium bismuth iodides, many different types of inorganic anion exist (e.g. with BiX_6, Bi_2X_8, Bi_4X_{16}, Bi_3X_{10}) and can often be found as competing phases in products.[1]

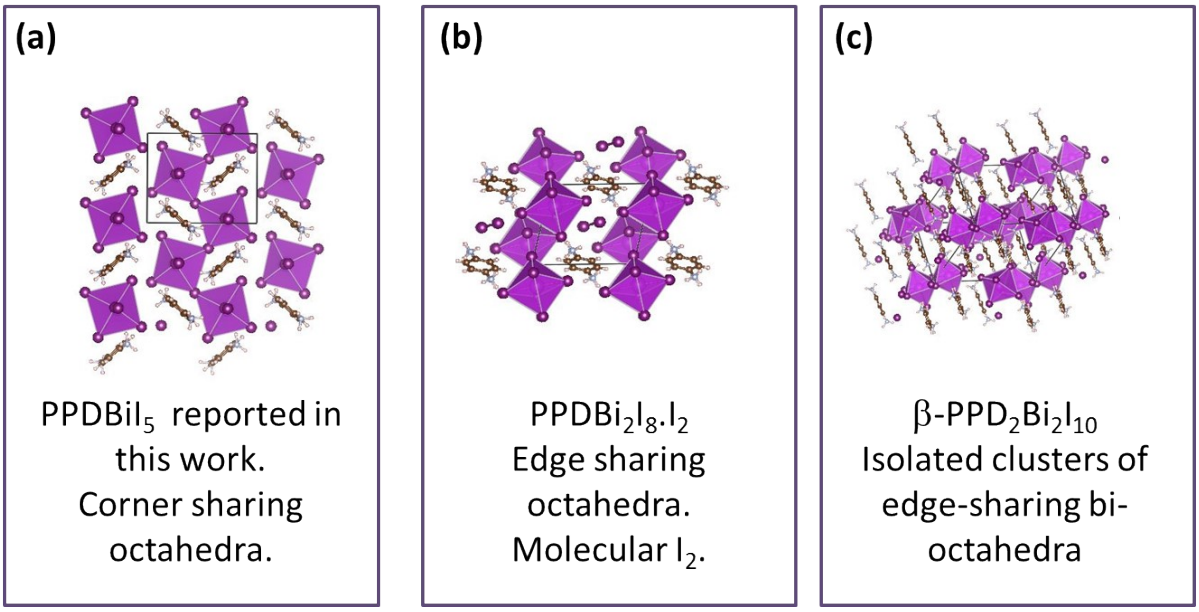

Figure S4: Other structures in the PPD-Bi-I system (a) (PPD)BiI_5 reported in this work, (b) (PPD)$Bi_2I_8 \cdot I_2$, (c) β-(PPD)$_2Bi_2I_{10}$.

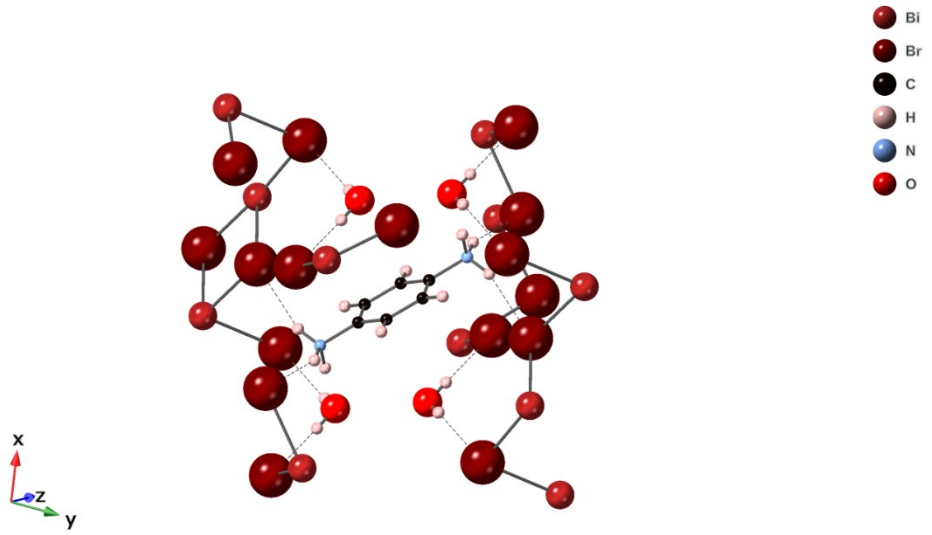

Figure S5: Role of hydrogen bonding in (PPD)$[BiBr_4]_2 \cdot 2H_2O$. Hydrogen bonding interactions between NH_3^+ and $BiBr_6$ and H_2O and $BiBr_6/NH_3^+$ group are clearly indicated.

Figure S6 shows the Pawley fit to the PXRD data for the PPD-Bi-Br sample. (PPD)$[BiBr_4]_2 \cdot 2H_2O$ (2) is present as the major phase with unit cell parameters a = 7.2547(7) Å, b = 12.1748(6) Å, c = 12.839644(9) Å, β = 97.793(6) ° (space group $P2_1/c$). A small amount of an impurity phase, the brominated version of β-$(PPD)_2Bi_2I_{10}$ was identified in the diffraction pattern with monoclinic unit cell parameters a = 10.789(3) Å, b = 12.330(3) Å, c = 14.267(7) Å , β = 110.49(3)°. This is a new material and will be discussed further in a future publication.

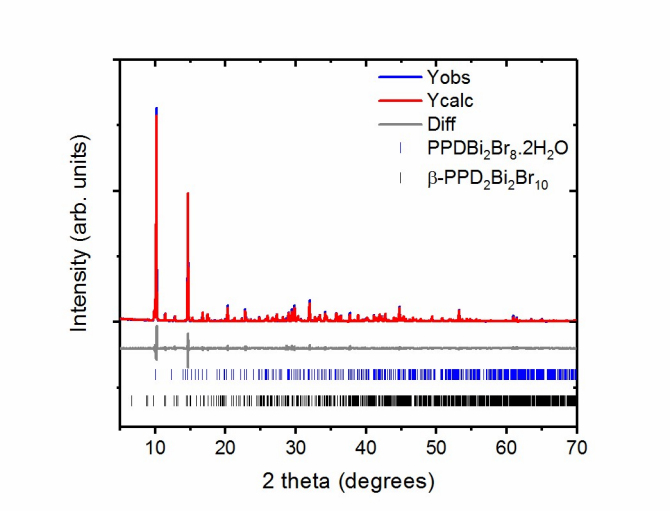

Figure S6: Pawley fit to PXRD data obtained for the PPD-Bi-Br sample. Blue tick marks represent the $(PPD)[BiBr_4]_2 \cdot 2H_2O$ phase and the black ticks represent a monoclinic Br containing phases, isostructural to β-$(PPD)_2Bi_2I_{10}$.

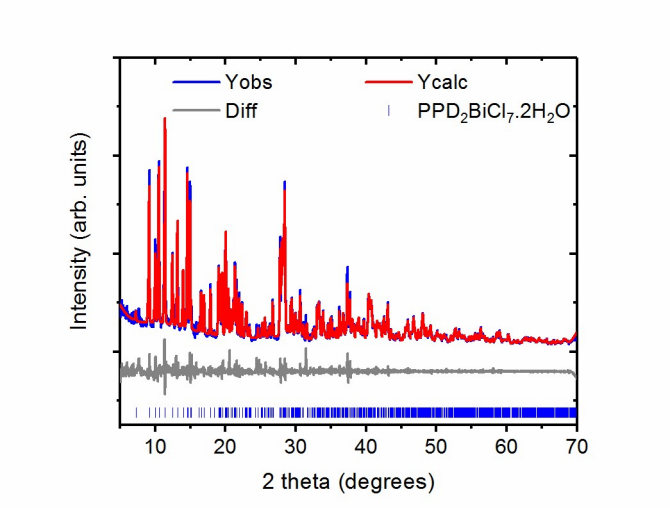

Figure S 7: Pawley fit to PXRD data obtained for the PPD-Bi-Cl sample. Blue tick marks represent $(PPD)_2BiCl_7 \cdot H_2O$.

Figure S7 shows the Pawley fit to the PXRD data obtained on the PPD-Bi-Cl sample. The data can be indexed to the same triclinic unit cell obtained for $(PPD)_2BiCl_7 \cdot H_2O$ (3) during the single crystal experiment with cell parameters, a = 9.5373(8) Å, b = 10.3450(8) Å, c = 13.5112(11) Å, 98.766(5)°, 11.072(7)°, 104.856(6)° (space group P-1).

Table S 2: X-Bi-X bond angles for $(PPD)BiI_5$, $(PPD)[BiBr_4]_2{\cdot}2H_2O$, $(PPD)_2BiCl_7{\cdot}H_2O$ and β-$(PPD)_2Bi_2I_{10}$

$(PPD)BiI_5$	$(PPD)[BiBr_4]_2{\cdot}2H_2O$	$(PPD)_2BiCl_7{\cdot}H_2O$	β-$(PPD)_2Bi_2I_{10}$
98.522(17) °	95.82(4) °	91.23(9) °	88.85(7) °
91.162(17) °	88.22(3) °	90.41(9) °	89.85(8) °
89.918(17) °	93.88(3) °	87.67(8) °	90.26(7) °
91.583(16) °	90.42(3) °	94.29(9) °	91.13(6) °
89.408(15) °	91.55(3) °	87.50(9) °	91.46(6) °
177.241(19) °	174.51(3) °	173.33(9) °	88.54(6) °
86.124(16) °	91.84(3) °	177.19(8) °	90.69(7) °
173.479(17) °	172.26(3) °	89.49(9) °	89.17(7) °
94.579(17) °	87.43(3) °	86.90(8) °	87.38(6) °
85.878(15) °	87.30(3) °	88.46(8) °	90.77(6) °
169.508(18) °	173.81(3) °	93.79(8) °	90.46(6) °
91.913(16) °	88.59(3) °	170.59(8) °	91.55(7) °
89.931(16) °	87.15(3) °	84.35(8) °	178.64(8) °
87.418(15) °	93.81(3) °	100.03(9) °	177.35(7) °
83.387(8) °	83.86(3) °	85.12(8) °	177.84(6) °

The stability under ambient conditions was confirmed by taking the PXRD of samples immediately after preparation and a month after initial synthesis for compound β-$(PPD)_2Bi_2I_{10}$ which indicated that no prominent change in the diffraction pattern of this compound had occurred. A similar comparison was made for compounds $(PPD)[BiBr_4]_2{\cdot}2H_2O$ and $(PPD)_2BiCl_7{\cdot}2H_2O$, the PXRD being taken again after eight months. No extra phases were observed in the diffraction pattern suggesting that these phases are relatively stable upon storing in air for several months (Figure S8).

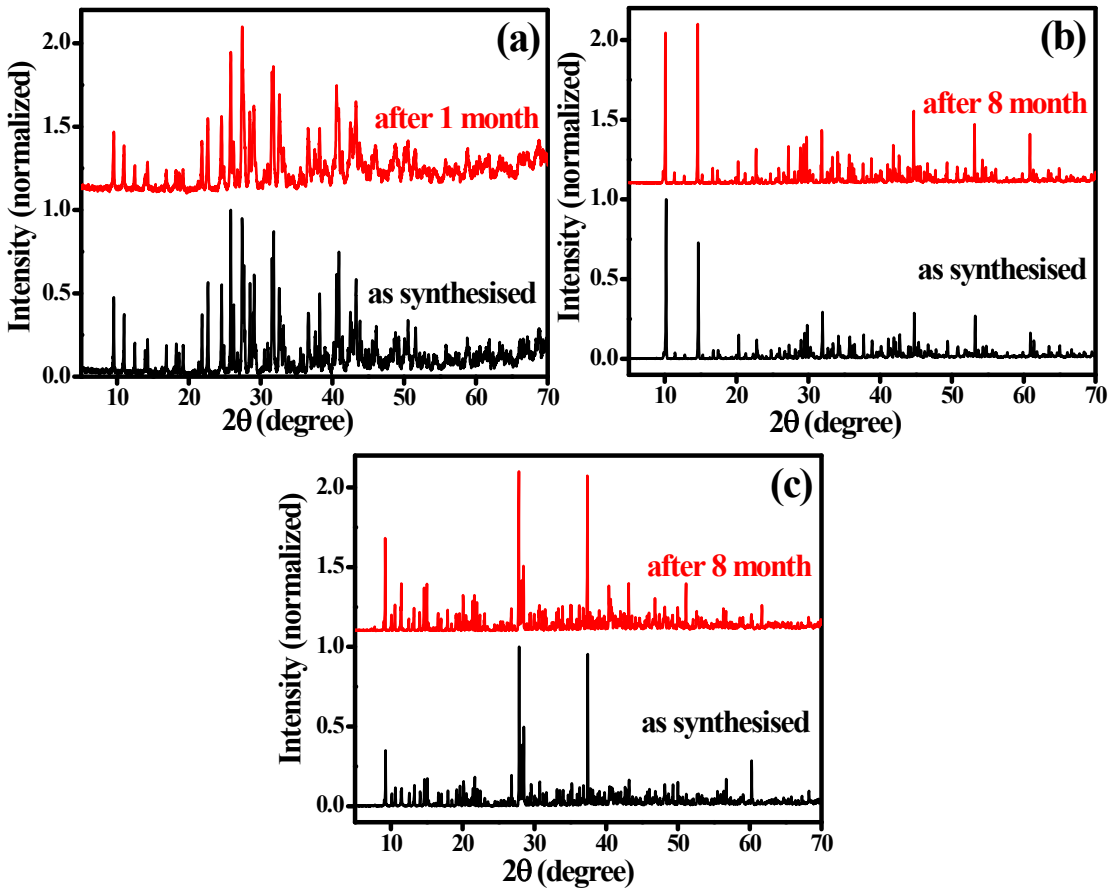

Figure S 8: PXRD patterns of compounds (a) β-$(PPD)_2Bi_2I_{10}$, (b) $(PPD)[BiBr_4]_2 \cdot 2H_2O$ and (c) $(PPD)_2BiCl_7 \cdot H_2O$.

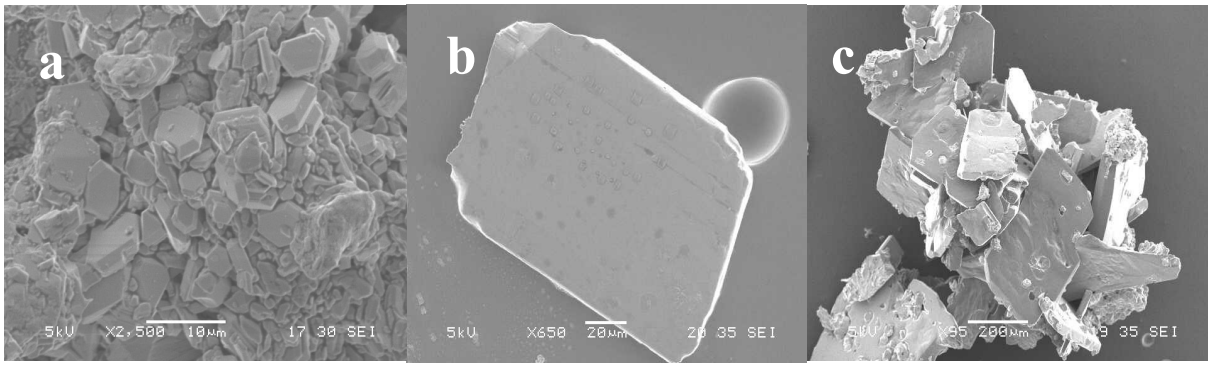

Figure S 9: SEM images of compounds (a) β-$(PPD)_2Bi_2I_{10}$, (b) $(PPD)[BiBr_4]_2 \cdot 2H_2O$ and (c) $(PPD)_2BiCl_7 \cdot H_2O$.

The FTIR spectra of β-$(PPD)_2Bi_2I_{10}$, $(PPD)[BiBr_4]_2 \cdot 2H_2O$ and $(PPD)_2BiCl_7 \cdot 2H_2O$ are shown in Figure S10 and Table S2 summarizes the characteristic vibrational frequencies of

these materials. The IR absorption bands at 3481, 3508 and 3529 cm^{-1} were assigned to the N-H symmetric stretch. Bands at 2836, 2877 and 2890 cm^{-1} were associated with the aromatic ring C-H stretch. The N-H bending deformations were credited to the bands at 1574, 1588 and 1561 cm^{-1}. The presence of vibrational frequencies at 1493 and 1495 cm^{-1} are due to the aromatic ring C=C bonds. The vibrational peaks at 1105 and 1118 cm^{-1} correspond to the deformation of C-H bonds. The frequencies at 795, 822 and 811 cm^{-1} were assigned to the NH and NH_2 deformations. The absorption peaks at 475, 489 and 499 cm^{-1} were assigned to the metal–halogen bonds.

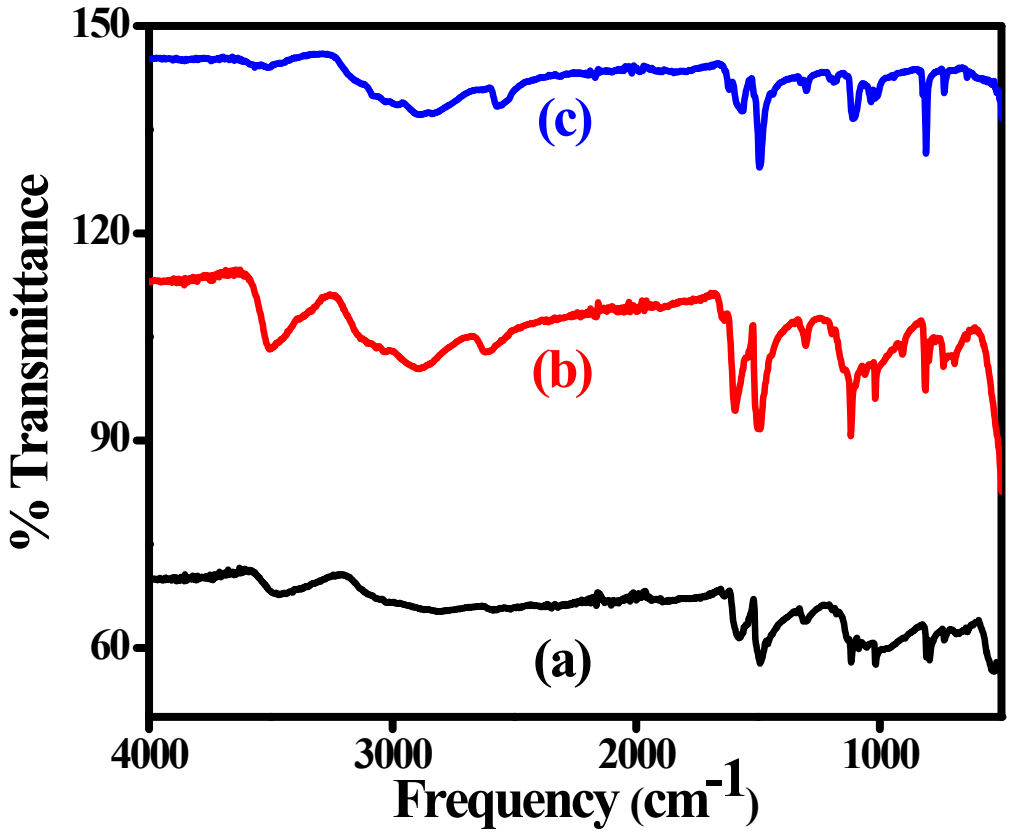

Figure S 10: FTIR spectra of (a) β-$(PPD)_2Bi_2I_{10}$, (b) $(PPD)[BiBr_4]_2 \cdot 2H_2O$ and (c) $(PPD)_2BiCl_7 \cdot 2H_2O$.

Table S3 Vibrational frequencies of β-$(PPD)_2Bi_2I_{10}$, $(PPD)[BiBr_4]_2 \cdot 2H_2O$ and $(PPD)_2BiCl_7 \cdot 2H_2O$.

	β-$(PPD)_2Bi_2I_{10}$	$(PPD)[BiBr_4]_2 \cdot 2H_2O$	$(PPD)_2BiCl_7 \cdot H_2O$
N-H symmetric stretch	3481	3508	3529
C-H stretch	2836	2877	2890
N-H bonding	1574	1588	1561
C-C aromatic	1493	1493	1495
C-H bending	1118	1105	1118
NH and NH_2	795	822	811
Bi-X	475	489	499

References

1. A. N. Usoltsev, M. Elshobaki,S. A. Adonin, L. A. Frolova, T. Derzhavskaya, P. A. Abramov, D. V. Anokhin, I. V. Korolkov, S. Yu. Luchkin, N. N. Dremova, K. J. Stevenson, M. N. Sokolov, V. P. Fedinad and P. A. Troshin, *J. Mater. Chem. A*, 2019, 7, 5957-5966.